The behaviour of SiO_2 content in strength development of alkali- activated red mud slag paste under ambient condition

Dr. Lasyamayee Garanayak

Asst. Professor of Civil Engineering Department, ITER College, Bhubaneswar.

Abstract

The excess demand for cement in construction era is relevant compatible to maxima utilization of industrial solid waste as an alternation of binding material. Since disposal of red mud turns to major environmental issue for its alkalinity nature, so this research was to evaluate the viability of red mud as a cementitious material. This type of material was developed by addition of granulated slag and red mud with three different proportion i.e. 30/70, 50/50, and 70/30. Those solid compositions were activated with the low concentration of alkali solution prepared by sodium hydroxide pellet and sodium silicate powder varying as mole proportion of SiO_2-Na_2O from 0 to 1.5 mole. Best compressive strength values were obtained by $ARSC_{50}$ containing 50% slag and 50% red mud but activated by $SN_{1.5}$ with the value 90.1MPa after 60 days of curing age in ambient condition. Hydration characteristics of $ARSC_{50}$ were observed by XRD, SEM. Ettringite and amorphous C-S-H gel are the prime factors of strength development of ARSC. This paper provides a major solution of utilization of red mud and preservation of energy and natural sources.

Key words- Red mud, sodium hydroxide, sodium silicate powder.

Introduction

The rapid increase in demand for building materials, as well as industrial products, is owing to the increase in population and of infrastructure development. But, accumulation of unmanaged industrial wastes in developing countries creates environmental distress like water pollution by leachate process, air pollution by dust process which directly and indirectly affected the entire life of the living creature. Hence, an acute shortage of suitable materials, environmental pollution, and damage to economic resources are the necessities and encouraging the development of useful construction materials from industrial waste materials. Recycling of waste products in construction industries can produce cost-effective building materials, with less consumption of energy, enhancing the green construction and economic design sectors. In comparison to other building materials, Portland cement has become more popular due to its versatility, durability, economical, relatively used low embodied the energy and manufactured from a locally available material (Juenger *et al.* 2011). But the sustainability of the cement industry, in the long run, is an issue for high-energy consumption, an excess of greenhouse gases and the use of natural resources. The total energy requirement consists of thermal energy for burning of limestone and sand to produce clinker and electrical energy for grinding of raw material, coal, and clinker to produce fine cement (Madlool *et al.* 2011). According to research categories, estimated value of global emission of CO_2 in 2016 was 1.45 + 0.20 Gt during manufacture of Ordinary Portland cement (OPC) (Luukkonen *et al.* 2018). Hence, growth of green

environment is the major concern towards production of sustainability of construction material using industrial by-product by complete replacement of cement (Ahmari *et al.* 2012).

In technology world, production of alkali-activated material or geopolymer is now one of the advantageous binding material compared to OPC for reduction of CO_2 (Luukkonen *et al.* 2018). It is synthesized by alkali activating Si and Al-rich materials which result to form of polycondensing tetrahedral silica and alumina (Zhang *et al.* 2014). Example of major materials containing aluminosilicate are granulated blast furnace slag, fly ash, metakaolin, rice husk ash, red mud (Zhang *et al.* 2014; Zhang *et al.* 2017). Most commonly used type of activators are caustic alkali, silicate, carbonate and sulfate etc. (Zhang *et al.* 2017). Mechanical properties of alkali-activated material or geopolymer get affected by – (a) characteristics of raw materials that related to – Si/Al and Na/Al ratios, presence of amorphous compound, and particle size, (b) curing conditions related to – curing temperature, curing time, and curing humidity (Zhang *et al.* 2014). However, the reaction mechanism is differentiated as (a) high calcium system dominated by calcium alumina silicate hydrate (C-A-S-H) gels with tobermorite-like structure, and (b) low calcium system dominated by alkali aluminosilicate (N-A-S-H) gels with pseudo-zeolitic structure (Zhang *et al.* 2017).

According to the report, the global annual production rate of RM is 120 million (Zhang *et al.* 2014). It requires a large disposal area i.e. about $1km^2$ for every five years after production of 1 million tons of alumina per year. Storage of excess red mud not only expensive but also causing the serious environmental problem (Ribeiro *et al.* 2012) due to presence of toxic material and alkali nature. RM has high water content with strong alkalinity varying with pH as 10.5 to 13 (He *et al.* 2013) due to use of excess alkali to extract alumina. The large demand for cement is compatible with excess deposition of industrial waste like red mud (Ribeiro *et al.* 2012) which can recovery to recycling, utilizing as economical beneficiary in technology world (He *et al.* 2013). Ground granulated blast furnace granulated slag, another industrial by-product of iron production. Annually worldwide deposition of granulated slag varies as 125 million tons (Approx.) (Elibol and Sengul, 2016). Presence of latent hydraulic type in it leads to production of cementitious properties (Elibol and Sengul, 2016). So, here slag is used in red mud as complete replacement of cement.

Environmental pollution the major issue can be fixed by developing low emitted carbon dioxide binder material. This study seeks to investigate the strength of cementless alkali paste in the ambient condition that provided by the combination of red mud and granulated slag at different proportion. Mix proportion of solid particles get activated by the combination of Na_2O and SiO_2 content of sodium hydroxide (NaOH) and sodium silicate powder (Na_2SiO_3). The intention of this study is relevant to develop the early strength alkali activated material using the low concentration of alkali solution and low consumption of water during the curing period. Microstructure analysis was investigated by SEM, XRD to clarify gel formation after alkali activation. Mechanical properties were examined by compressive strength test.

2. Experimental Procedure

2.1 Source Materials

The red mud (RM) was collected from National Aluminium Company Limited (NALCO), Damanjodi of Koraput District of Odisha, India. The ground granulated blast furnace slag (GGBS) was collected from Rourkela Steel Plant (RSP), Sundergarh district of Odisha, India. Oven dried both materials were crushed

ball mill and get sieved by 150µm to obtain the fine particles. Chemical compositions were determined by X-ray fluorescence analysis (XRF) instrument of the model named PANalytical Axios that shown in Table 1.

Table 1 Chemical composition of RM and GGBS

Oxide Weight (%)	**RM**	**GGBS**
SiO2	9.75	32.44
Al2O3	19.10	17.06
Fe2O3	55.62	0.40
CaO	1.64	34.75
MgO	0.21	11.22
K2O	0.19	0.93
Na2O	9.12	0.24
TiO2	3.24	0.81
P2O5	0.20	-
SO3	0.29	-

Particle size distribution (PSD) of both 150µm pass RM and GGBS were tested by laser diffraction analyser of model name -MASTERSIZER S, Malvern, UK that in Figure 1. Those were expressed in terms of volume percentage and cumulative volume percentage. The characteristic particle diameters X10, X50, and X90 are described in terms of particle having 10%, 50% and 90% of the particles finer than this size, respectively. Here, characteristic particle diameters X10, X50, and X90 of RM were 0.83, 13.72 and 75.94 µm, respectively. Similarly, GGBS were obtained as 2.59, 25.36 and 109.59 µm respectively. It confirmed that 60% of particles were finer than 45 µm. It was considered that in the alkali-activated system, granulated slag reacts very slowly for a particle size above 20 µm and react completely within 24h (approx.) for a particle size of below 2 µm (Yusuf *et al.* 2014). According to the author, fineness of slag leads to better strength at early ages but decreases the setting time (Wang *et al.* 1994). On comparison of the base materials, RM was found to be finer than GGBS.

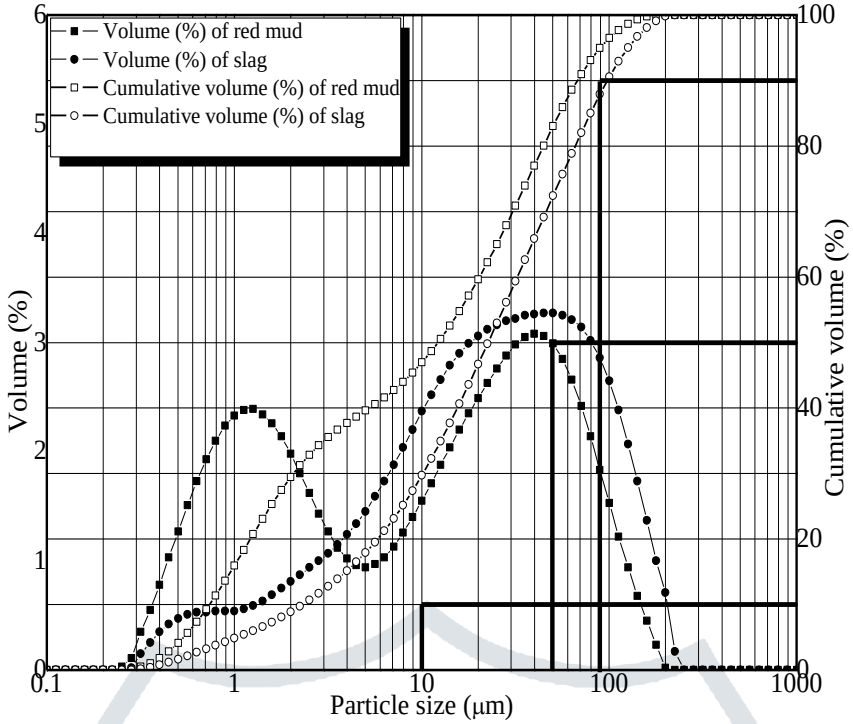

Figure 1 Particle size distribution of RM and GGBS

2.2 Alkali activators

In the present study two sodium based activators, named as sodium hydroxide also named as caustic soda or white soda and sodium silicate or water glass were used. Sodium hydroxide pellets of EMPLURA, Merck Socialization, and > 97% purity) and sodium silicate powder ($Na_2SiO_3.9H_2O$) of LOBA Chemie, Extra pure sodium metasilicate were used in this study. Both alkalies were prepared as per mole combination of SiO_2 and Na_2O content using distilled water. Activator was prepared one day prior to the sample casting to avoid exothermic reaction and maintain proper fusion reaction. Table 2 shows the mole content of chemical used which were notified as SN mole. Here S represents to SiO_2 and N refers to Na_2O.

Table 2 Chemical composition of alkali activator

Activator designation SN_{mole}	**SiO_2 (mole) proportion**	**Na_2O (mole) proportion**
SN_0	0	1.5
$SN_{0.5}$	0.5	1.5
SN_1	1	1.5
$SN_{1.5}$	1.5	1.5

2.3 Synthesis procedure

Oven dried RM and GGBS were mixed with three different proportions i.e., 30/70, 50/50, and 70/30 as weight percentages which were signified as RS_{30}, RS_{50}, and RS_{70} respectively. After addition with the prepared alkali solution, product samples were identified as alkali activated red mud slag cement material and indicated as $ARSC_{30}$, $ARSC_{50}$, and $ARSC_{70}$. The mixture of solid and solution was kept as 0.2 for $ARSC_{30}$, $ARSC_{50}$, and $ARSC_{70}$ respectively. Prepared ARSC paste of different proportion was immersed in the cube of 50 x 50 x 50 (mm^3) for one day to get settled at room temperature following ASTM standard

C109/C109M-13. Solid and solution mix proportion were shown in Table 3. However, the key chemical ratio of the mixture as shown in Table 4.

Table 3 Mix design proportion of alkali activated paste

Sample type	Mix proportion by mass (Unit: g)		
	RM	GGBS	Activator
$ARSC_{30}$	300	700	200
$ARSC_{50}$	500	500	200
$ARSC_{70}$	700	300	200

Table 3 Key chemical ratio of mixture

Categories	Sample type	Activator	SiO_2/Al_2O_3	SiO_2/Na_2O
I	ARS_{30}	S_0	1.45	1.39
	$ARSC_{50}$		1.17	1.05
	$ARSC_{70}$		0.9	0.75
II	$ARSC_{30}$	$S_{0.5}$	1.60	2.51
	$ARSC_{50}$		1.32	1.82
	$ARSC_{70}$		1.04	1.30
III	$ARSC_{30}$	S_1	1.66	3.39
	$ARSC_{50}$		1.37	2.38
	$ARSC_{70}$		1.10	1.66
IV	$ARSC_{30}$	$S_{1.5}$	1.69	4.11
	$ARSC_{50}$		1.40	2.80
	$ARSC_{70}$		1.12	1.92

2.4 Curing condition and Testing ages

After settled, paste samples were removed from the mould and kept in the oven at 60°C for 24 h to initiate hardened condition. To avoid moisture loss, each sample was wrapped by cling film during the period of oven curing and considered as the 1st phase of curing. Then each sample proceeded to the 2nd phase of curing and considered as the ambient condition. In this stage, wrapped free samples were kept at room temperature up to different testing ages i.e. 3, 7, and 28, and 60 days. Then each sample was used to measure the compressive strength through the compressive strength testing machine.

3. Result and Discussion

3.1. Compressive strength

In this section, the compressive strength of ARSC pastes is discussed which varies according to activator type, granulated slag proportion at the constant curing temperature. For particular solid proportion, compressive strength gets increased with increase in the mole of SiO_2 content. But for the particular activator, strength get increased with increase in the percentage of slag content.

3.1.1 Effect of SiO_2/Na_2O ratio of activator

In this study, four alkali solution is used as the activator to initiate the geopolymerization in between RM and GGBS. Table 2 shows the chemical composition of activator which is the combination of sodium hydroxide and sodium silicate solution but with low concentration. Most of the articles have explained the formation of geopolymer product with high concentration of NaOH (Phair and van Deventer, 2002; Bakri *et al.* 2012; Ryu *et al.* 2013; Mijarsh *et al.* 2015), Na_2SiO_3, or combination of NaOH solution and liquid Na_2SiO_3 (Karakoç *et al.* 2014; Phoo-Ngernkham *et al.* 2015). But new research is involved with sodium silicate powder (Yang *et al.* 2008). This study involves to developed alkali product by using the low concentration of the combination of NaOH solution and powdered Na_2SiO_3. Figure 2 shows the effect of low concentrated activator on the compressive strength of ARSC paste at different curing ages. It is observed with high early strength gain with increasing weight percentage of GGBS proportion. Strengths are observed as 41.53, 66.14, 77.97, 83.45MPa with $ARSC_{30}$; 43.39, 51.78, 68.79, and 90.1MPa with $ARSC_{50}$; 34.69, 39.16, 43.43, 61.49MPa with $ARSC_{70}$ after 60 days of curing ages. Those strengths are varied with the aforementioned activators i.e., SN_0, $SN_{0.5}$, SN_1, and $SN_{1.5}$ respectively. Although high strength is observed by the $SN_{1.5}$ activator in three different weight proportion of RM and GGBS, it is maximum with ARSC50 than other two alkali paste. This strength can be explained of increase components of silica content in alkali solution and

Increase strength can be explained as the effect of silica content which is present both in alkali solution and solid composite (RM+GGBS).

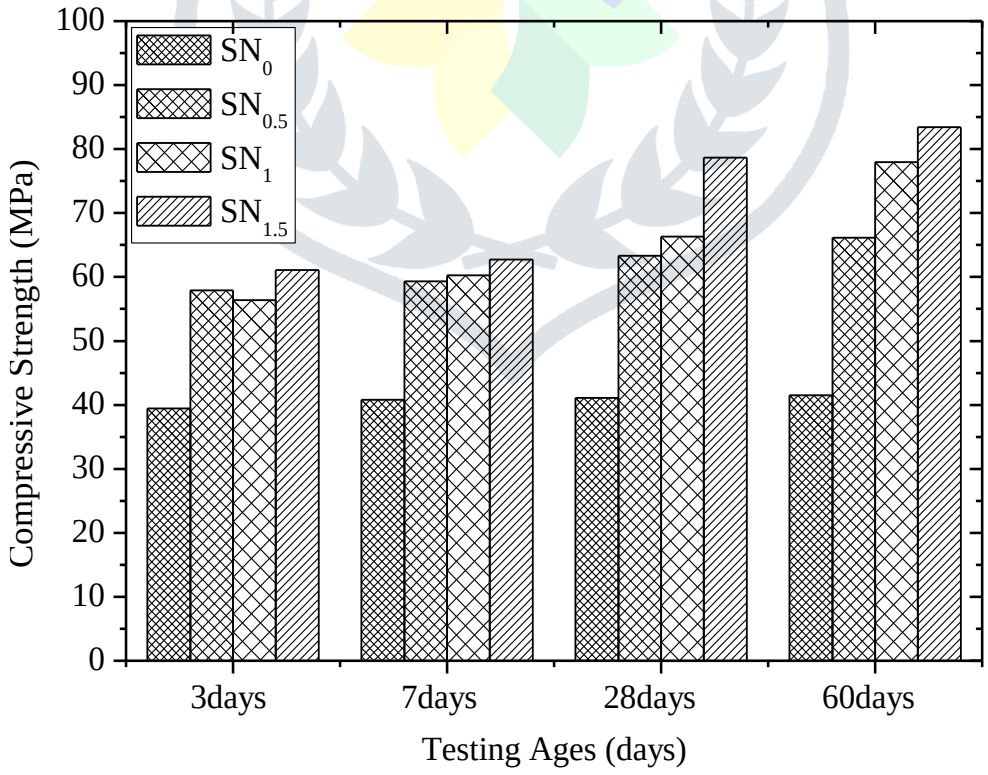

(a)

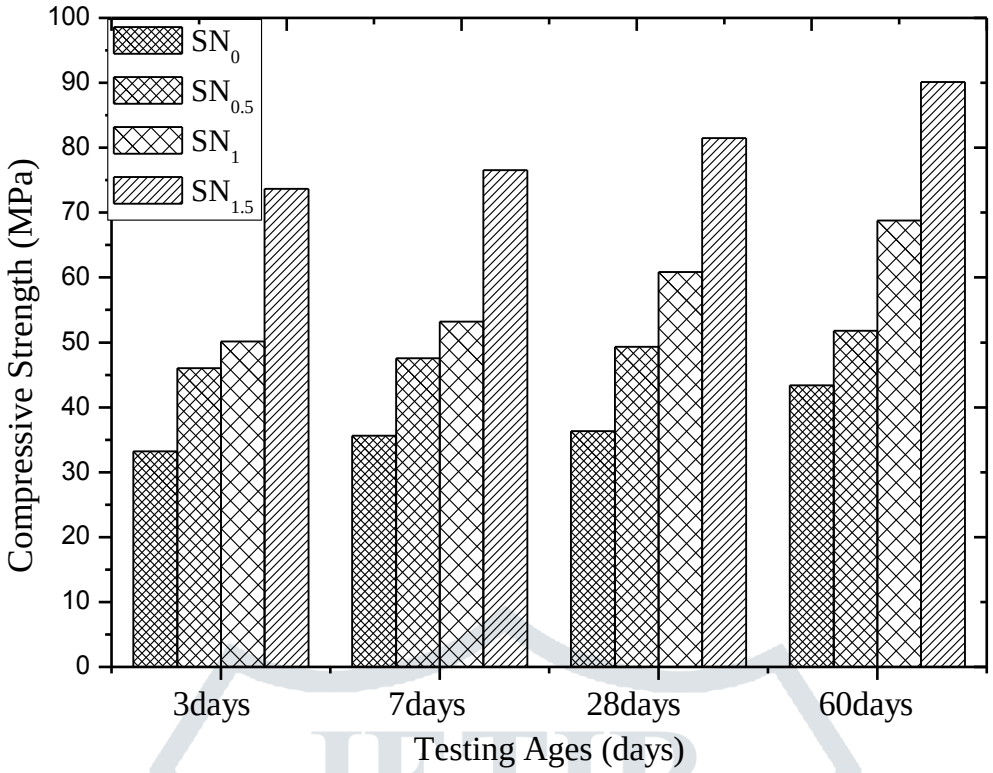

(b)

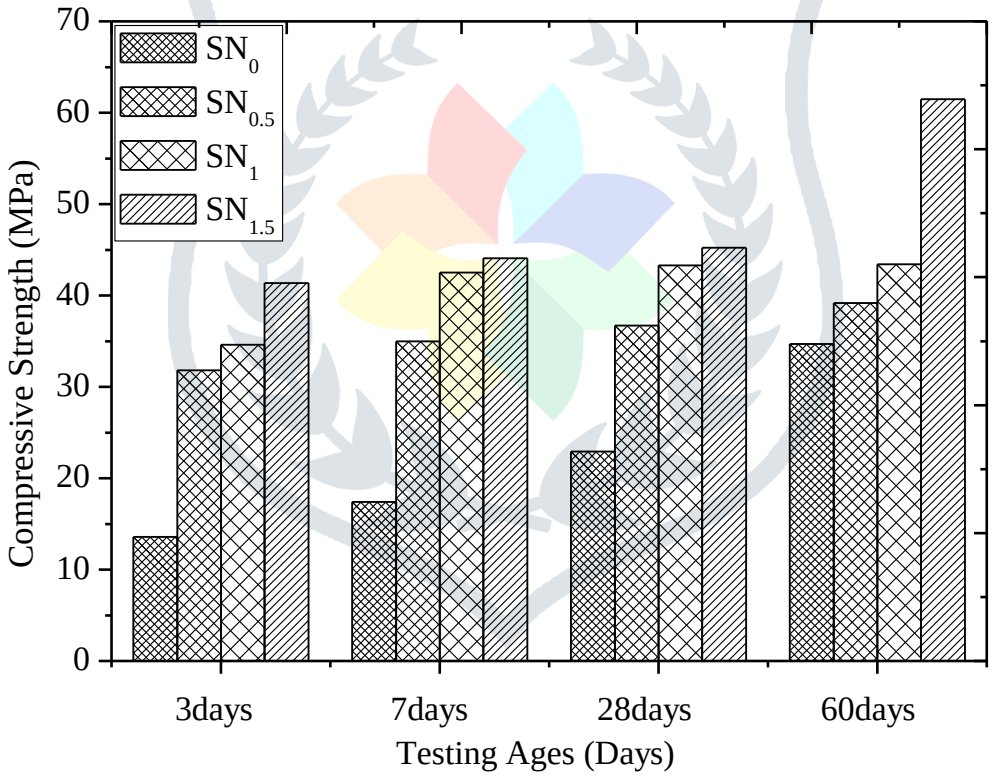

(c)

Figure 2 Effect of alkali activator on compressive strength (a) $ARSC_{30}$, (b) $ARSC_{50}$, and (c) $ARSC_{70}$

3.1.2 Effect of SiO_2/Na_2O ratio of alkali paste

Different activating solution i.e. SN_0, $SN_{0.5}$, SN_1, and $SN_{1.5}$ are varied with increase the mole content of SiO_2 from 0 to 1.5 mole, at constant 1.5 moles of Na_2O. Figure 2 presents the results of the analysis of the effect of SiO_2 of alkali-activated paste on compressive strength per testing ages. In addition of increase slag content and increase the SiO_2 content of alkali solution leads to high early compressive strength. In particular, 60 days strengths are observed as 41.53, 43.39, 34.69Mpa by 1.39, 1.05, and 0.75 SiO_2/Na_2O ratio of ARSC paste after activated by SN_0; 66.14, 51.78, 39.16MPa by 2.51, 1.82, 1.30 SiO_2/Na_2O ratio of ARSC

paste after activated by $SN_{0.5}$; 77.97, 68.79, 43.43MPa by 3.39, 2.38, 1.66 SiO_2/Na_2O ratio of ARSC paste after activated by SN_1; 83.45, 90.1, 61.49MPa by 4.11, 2.80, 1.92 SiO_2/Na_2O ratio of ARSC paste after activated by $SN_{1.5}$. Such results can be explicated by the activation reaction of internal Si and Al components of the solid composite materials. Those components are developed with breakage of glassy content (Ryu *et al.* 2013) of GGBS and RM after the geopolymerization process of alkali solution. It leads to the formation of high alkalinity and increases the mole content of SiO_2 of prepared alkali paste. The suddenness of reaction in presence of high curing temperature (Ryu *et al.* 2013) results to the early setting with the gain of early strength by $SN_{1.5}$ in compared to SN_0 due to proper polymerization between maximum mole content of SiO_2 of the alkali solution and presence of excess caustic soda (NaOH) in RM. This may be a better explanation of maximum strength gain by $SN_{1.5}$ in compared to other three alkali solution. Figure 2 shows the results of the analysis effect of the SiO_2 /Na_2O on compressive strength of prepared alkali paste after activated by the aforementioned four different activators with testing ages. It confirms that increase component of Si in activator and solid composition plays a major role to increase compressive strength, but S_0 and $S_{1.5}$ are found to be exceptional in $ARSC_{30}$ in compared to $ARSC_{50}$. This may be due to the improper reaction in compared to other two activators.

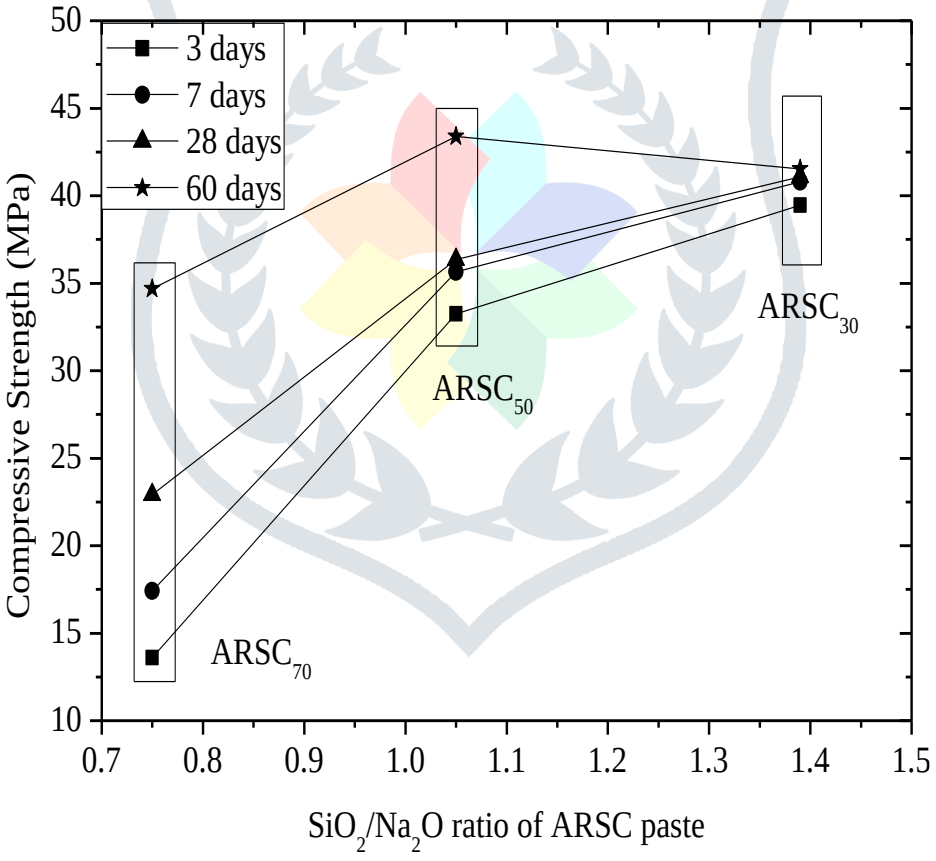

(a)

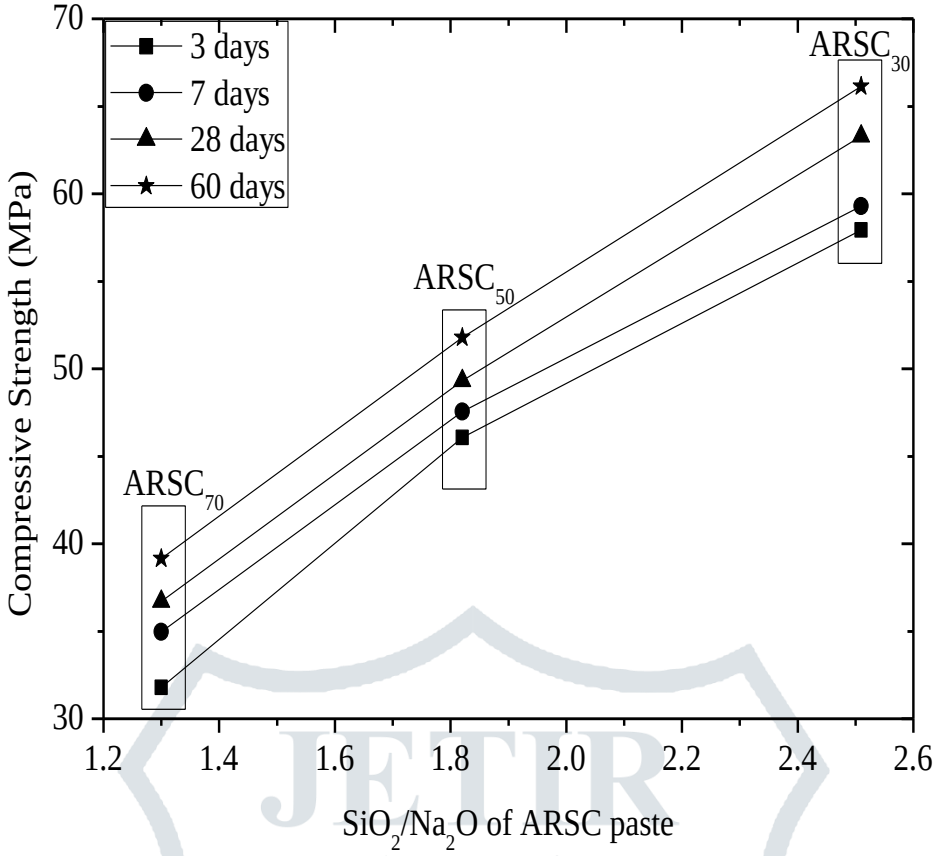
3 days
7 days
28 days
60 days
ARSC30
ARSC50
ARSC70
Compressive Strength (MPa)
70
60
50
40
30
1.2
1.4
1.6
1.8
2.0
2.2
2.4
2.6
SiO2/Na2O of ARSC paste

(b)

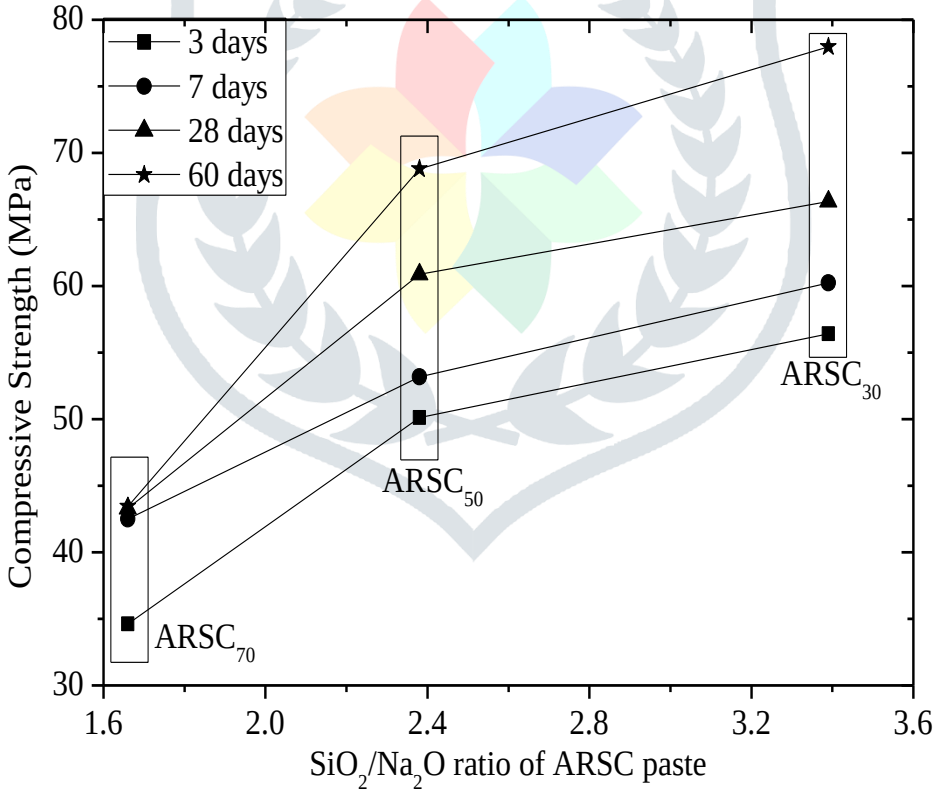
3 days
7 days
28 days
60 days
ARSC30
ARSC50
ARSC70
Compressive Strength (MPa)
80
70
60
50
40
30
1.6
2.0
2.4
2.8
3.2
3.6
SiO2/Na2O ratio of ARSC paste

(c)

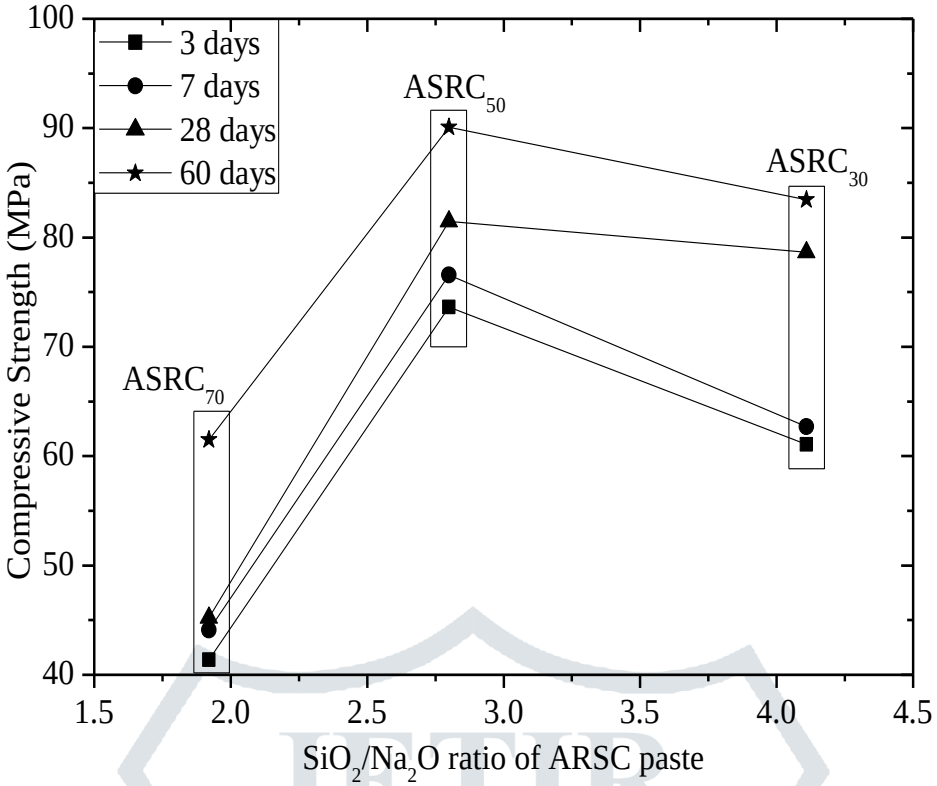

(d)

Figure 3 Effect of SiO_2/Na_2O ratio on compressive strength after activated by (a) SN_0, (b) $SN_{0.5}$, (c) SN_1, and (d) $SN_{1.5}$

3.2 X-ray diffraction (XRD)

XRD of each source material was carried out by XRD instrument of the model named Rigaku Ultima-IV, Japan using Cu Kα radiation. Scanning range was varied from 10 to 50 degrees with 0.05 as step size. Figure 4 (a) shows the XRD analysis of RM. It is observed to have compounds like gibbsite ($Al(OH)_3$), hematite (Fe_2O_3), quartz (SiO_2), mullite ($Al_6O_{13}Si_2$), calcite ($CaCO_3$), goethite ($Fe_2O_3.2H_2O$), sodalite ($Al_6Cl_2Na_8O_{24}Si_6$), and cancrinite ($Na_6Ca_2Al_6Si_6O_{24}(CO_3)_2 .2H_2O$). Most of the iron is present in the form of hematite and goethite. Kaya et al. (2016) observed that gibbsite and hematite are the major compounds followed by mullite, calcite, goethite, and perovskite. Figure 4 shows the XRD image of GGBS that contain minerals, Akermanite (Ca_2Mg [Si_2O7]), Gehlenite (Ca2Al [AlSiO7]), Wagnerite $(MgFe)_2PO_4F$, and Melilite $(Ca, Na)_2(Al, Mg, Fe2+)$ [(Al, Si) SiO_7]. Wide humps are observed between 20 to 40°, centred at 30° and conform to a significant number of amorphous phases. The presence of amorphous structure leads to the development of high pozzolanic activity and binding property which conforms in RSP slag (Karakurt and Topçu, 2012).

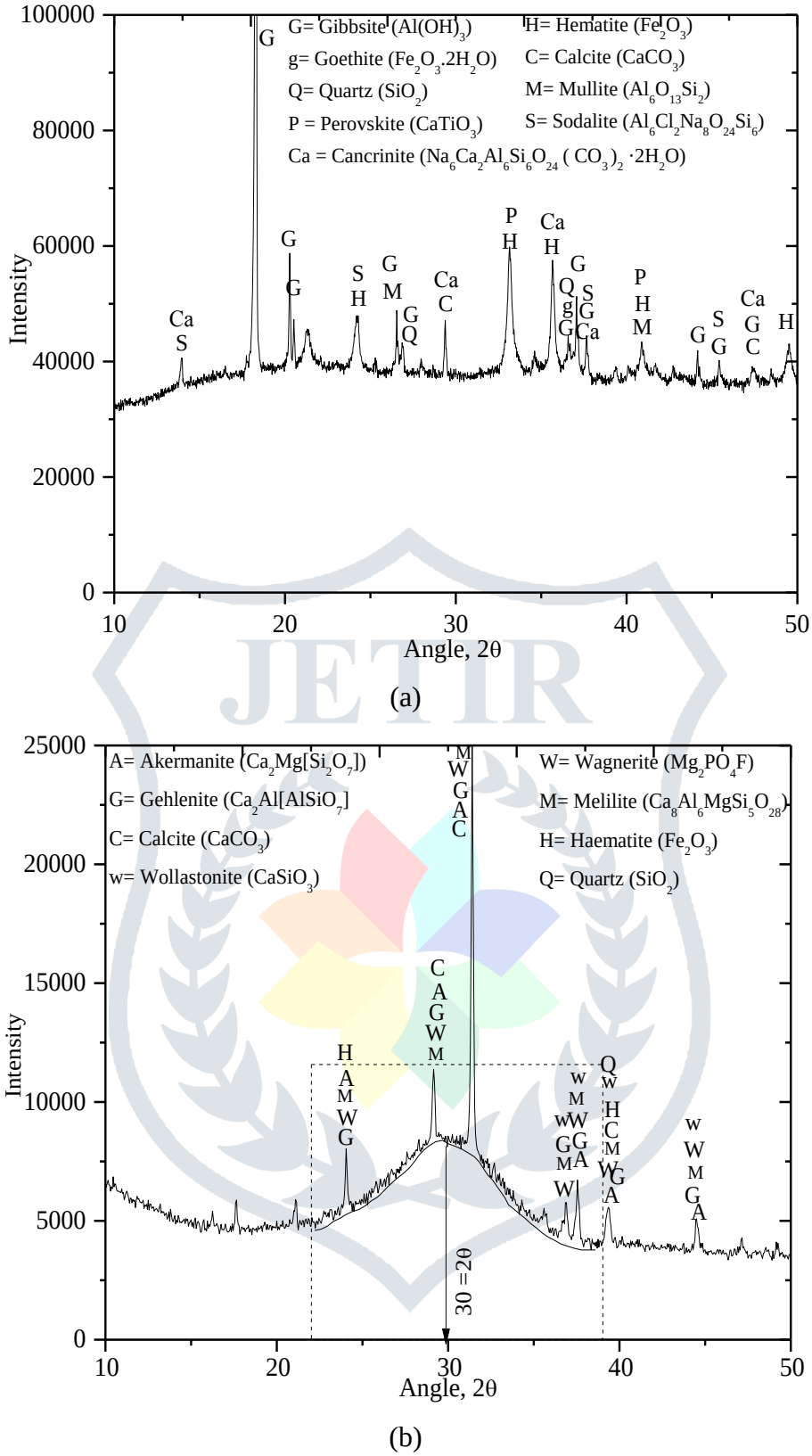

Figure 4 XRD of (a) RM and (b) GGBS

For maximum strength, XRD analysis is observed by $ARSC_{50}$ after 28 days of curing age that activated by said activator as shown in Figure 5. The main products are obtained by the geopolymerization process in between alumina-silicate substances and amorphous structure of the raw materials in presence of alkali solution (Ryu *et al.* 2013). From the analysis, ettringite (Ca_6 Al_2 SO_4 $3(OH)_{12}$. $26H_2O$), CSH ($Ca_2SiO_4.H_2O$), calcite ($CaCO_3$) are obtained as the major compound. Presence of ettringite leads to increase the volume of hydrates, decrease the porosity and increase the strength (Bizzozero and Scrivener, 2015). Formation of ettringite due to the reaction of Ca and desolated Al and Si content (Guo *et al.* 2010). Ca

content of granulated slag reacted with dissolved silicate and aluminate species to form C-S-H gel (Guo *et al.* 2010). Presence of ettringite and C-S-H leads to strength development in $ARSC_{50}$ paste (Zhang et al. 2011).

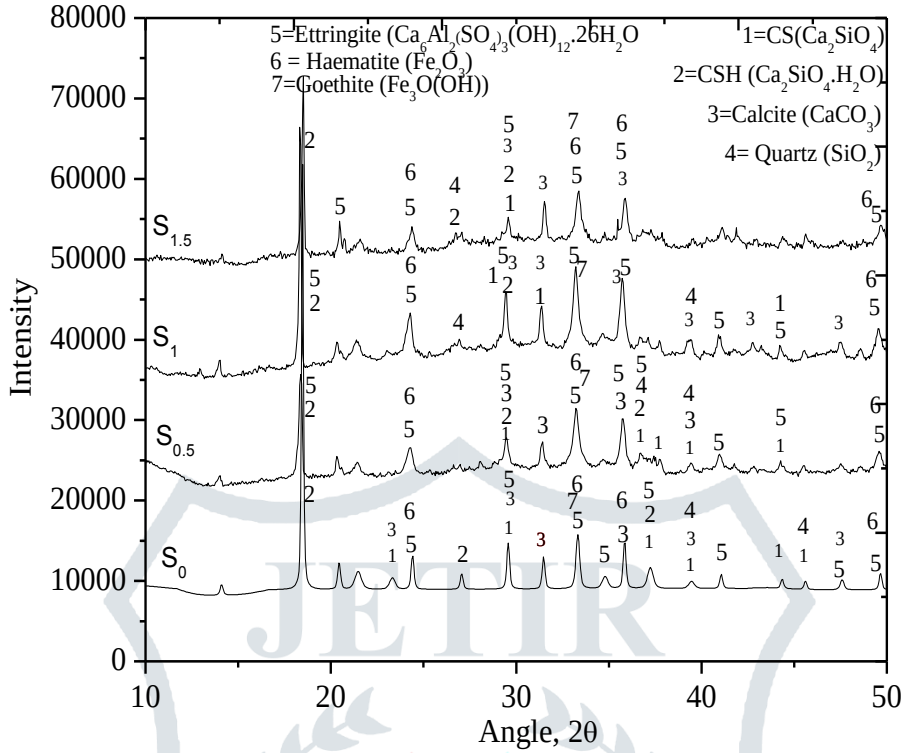

Figure 5 XRD image of ARSC50 after 28 days of curing age at different activator

3.3 Scanning electron microscopy (SEM)

The microstructure image of RM and GGBS were observed through SEM instrument of the model - JEOL JSM-6480LV. From Figure 6 (a), it is observed that RM are granular type consisting of a combination of irregular, round, cubic as well as prismatic structures. However, GGBS is observed as an angular shape with sharp edges, smooth surface that exhibits with irregular pattern (shown in Figure 6 (b)). Figure 7 shows the SEM image of $ASRC_{50}$ in an ambient curing condition activated by (a) SN_0, and (b) $SN_{1.5}$ activators. It observed with the flat plate-like structure of calcium – silicate hydrates (C-S-H) and few structures with the needle-like structure that may be due to the presence of ettringite. Hydration product of ettringite and the C-S-H gel is the reason for higher strength in alkali paste after ambient curing condition (Zhang *et al.* 2011).

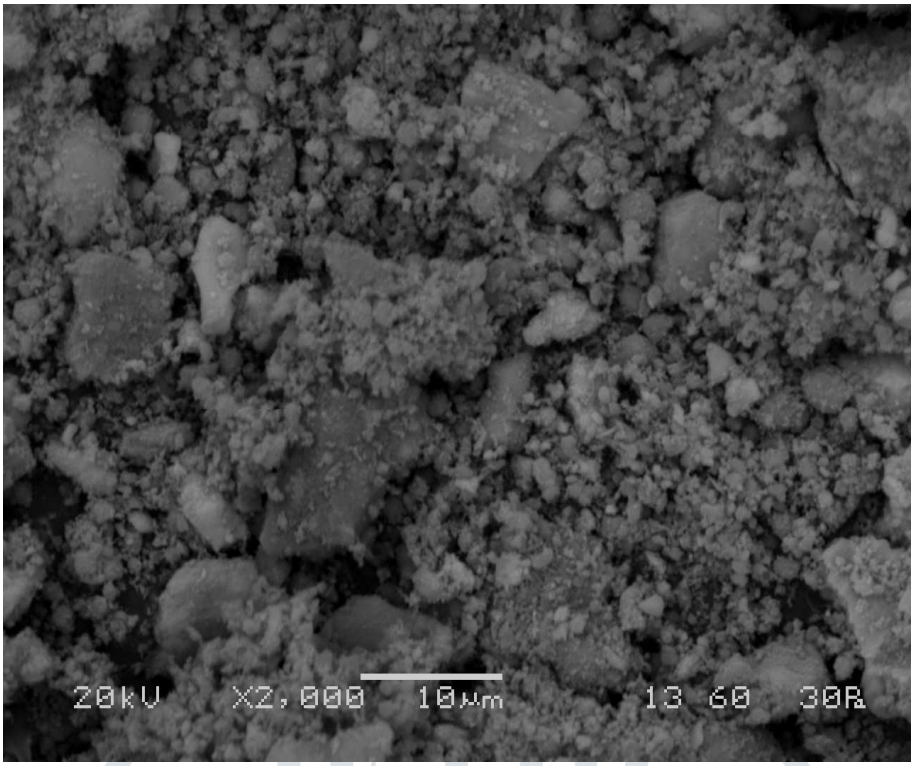

(a)

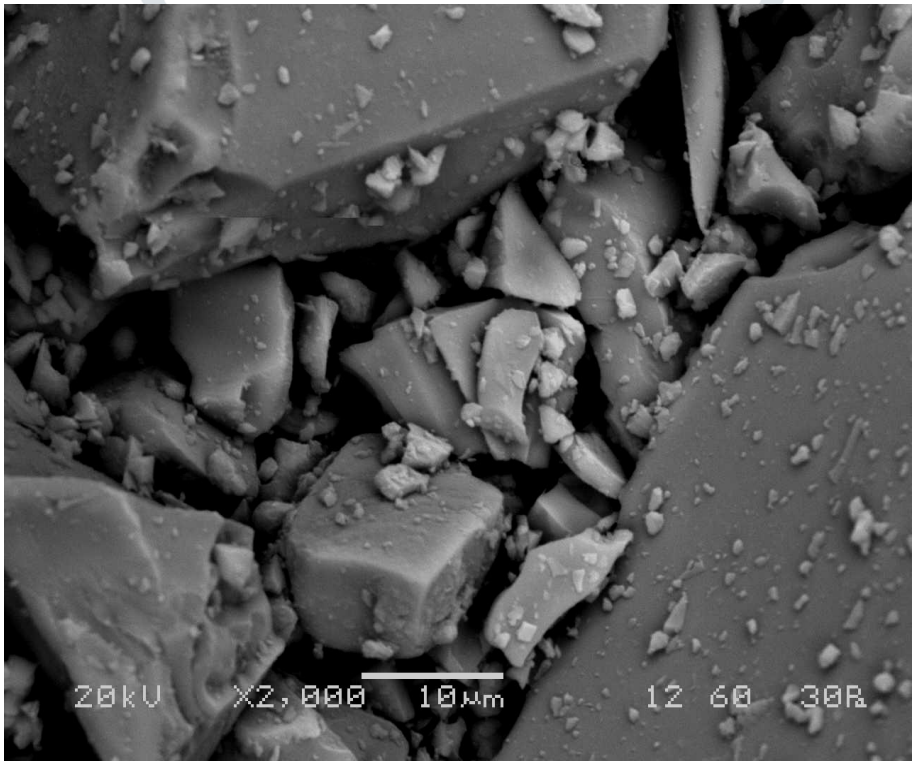

(b)

Figure 6 SEM image of (a) RM, and (b) GGBS

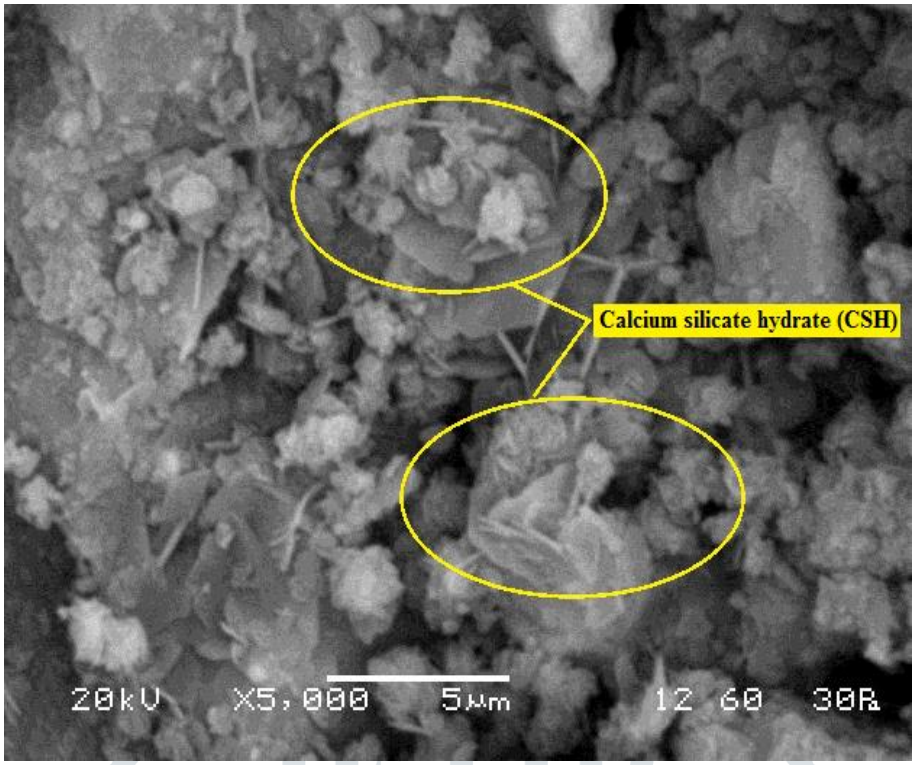

(a)

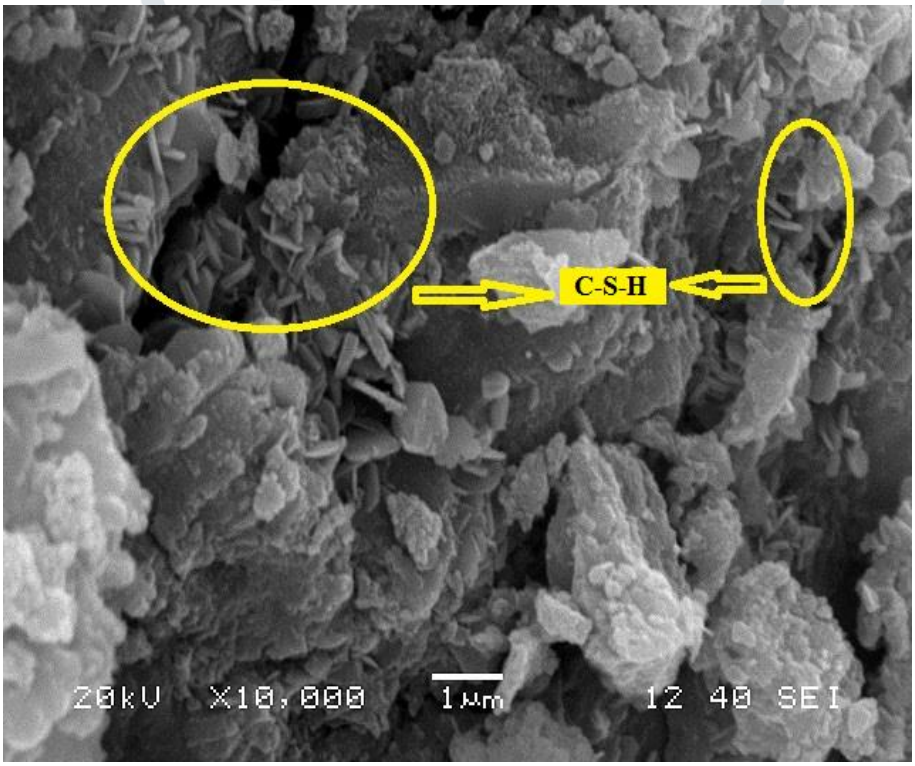

(b)

Figure 7 SEM image of $ARSC_{50}$ activated by (a) SN_0 and (b) $SN_{1.5}$

4. Conclusions

Following conclusion are drawn with alkali-activated red mud slag cementitious material

1. Addition of granulated slag improves the physical and mechanical properties.
2. Better strength is achieved due to fineness of red mud and slag which require least amount solution solid ratio.

3. $ARSC_{50}$ produced better strength in compared to $ARSC_{30}$ and $ARSC_{70}$.
4. $ARSC_{50}$ produced high compressive strength by $SN_{1.5}$ solution than other alkali solution.
5. Ettringite and C-S-H play as major contributor for strength development.
6. With increase the silica content in alkali solution, particle structure of C-S-H production turns to thicker than absence of silica content.
7. Early strength production in ARSC may resolve the issue of scarcity of water for less consumption of water during preparation of product material and no requirement of water during curing.

Reference

1. ASTM C109 / C109M – 13 Standard Test Method for Compressive Strength of Hydraulic Cement Mortars (Using 2-in. or [50-mm] Cube Specimens).
2. Luukkonen, T, Abdollahnejad, Z, Yliniemi, J, Kinnunen, P, and Illikainen, M. One Part of alkali – activated material: A review. Cement and Concrete 103 (2018) 21-34.
3. Ryu, GS, Lee, YB, Koh, KT, and Chung, YS. The mechanical properties of fly ash-based geopolymer concrete with alkaline activators. Construction and Building Materials 47 (2013) 409–418.
4. Mijarsh, MJA, Megat JMA, Ahmad, ZA. Effect of delay time and Na2SiO3 concentrations on compressive strength development of geopolymer mortar synthesized from TPOFA. Construction and Building Materials 86 (2015) 64–74.
5. Al Bakri, AMM, Kamarudin, H, Bnhussain, M, Rafiza, AR, Zarina, Y. Effect of Na2SiO3/NaOH ratios and NaOH molarities on compressive strength of fly-ash-based geopolymer. ACI Materials Journal 109:5 (2012) 503-508.
6. Yang, KH, Song, JK, Ashour, AF, Lee, ET. Properties of cementless mortars activated by sodium silicate. Available online at www.sciencedirect.com Construction and Building Materials 22:9 (2008) 1981–1989.
7. Karakoç, MB, Türkmen, I, Maraş, MM, Kantarci, F, Demirboła, R, Ułur TM. Mechanical properties and setting time of ferrochrome slag based geopolymer paste and mortar. Construction and Building Materials 72 (2014) 283–292.
8. Phoo-Ngernkham, T, Maegawa, A, Mishima, N, Hatanaka, S, Chindaprasirt, P. Effects of sodium hydroxide and sodium silicate solutions on compressive and shear bond strengths of FA-GBFS geopolymer. Construction and Building Materials 91 (2015) 1–8.
9. Phair, JW, Van Deventer, JSJ. Effect of the silicate activator pH on the microstructural characteristics of waste-based geopolymers. Mineral Engineering, 14: (3), pp. 289-304, 2001.
10. Juenger, MCG, Winnefeld, F, Provis, JL, Ideker, JH. Advances in alternative cementitious binders. Cement and Concrete Research 41 (2011) 1232–1243.
11. Zhang, J, Shi, C, Zhang, Z, Ou, Z. Durability of alkali-activated materials in aggressive environments: A review on recent studies. Construction and Building Materials 152 (2017) 598–613.
12. Madlool, NA, Saidur, R, Hossain, MS, Rahim, NA. A critical review on energy use and savings in the cement industries. Renewable and Sustainable Energy Reviews 15 (2011) 2042–2060.

13. Ribeiro, DV, Labrincha, JA, Morelli, MR. Effect of the addition of red mud on the corrosion parameters of reinforced concrete. Cement and Concrete Research 42 (2012) 124–133.
14. Zhang, M, El-Korchi, T, Zhang, G, Liang, J, Tao, M. Synthesis factors affecting mechanical properties, microstructure, and chemical composition of red mud-fly ash based geopolymers. Fuel 134 (2014) 315–325.
15. Bizzozero, J, Scrivener, KL. Limestone reaction in calcium aluminate cement - calcium sulfate systems. Cement and Concrete Research 76 (2015) 159–169.
16. Guo, X, Shi, H, Chen, L, Dick, WA. Alkali-activated complex binders from class C fly ash and Ca-containing admixtures. Journal of Hazardous Materials 173 (2010) 480–486.
17. Zhang, N, Liu, X, Sun, H, Li, L. Evaluation of blends bauxite-calcination-method red mud with other industrial wastes as a cementitious material: properties and hydration characteristics. Journal of Hazardous Materials 185 (2011) 329–335.
18. Ahmari, S, Zhang, L. Utilization of cement kiln dust (CKD) to enhance mine tailings-based geopolymer bricks. Construction and Building Materials 40 (2013) 1002–1011.
19. Ahmari, S, Ren, X, Toufigh, V, Zhang, L. Production of geopolymeric binder from blended waste concrete powder and fly ash. Construction and Building Materials 35 (2012) 718–729.
20. He, J, Jie, Y, Zhang, J, Yu, Y, Zhang, G. Synthesis and characterization of red mud and rice husk ash-based geopolymer composites. Cement & Concrete Composites 37 (2013) 108–118.
21. Elibol, C, Sengul, O. Effects of Activator Properties and Ferrochrome Slag Aggregates on the Properties of alkali-activated Blast Furnace Slag Mortars. Arabian Journal for Science and Engineering (2016) 41:1561-1571.